AIAA JOURNAL
Vol. 30, No. 6, June 1992

Renormalization Group Based Algebraic Turbulence Model for Three-Dimensional Turbomachinery Flows

K. R. Kirtley*
Sverdrup Technology, Inc., Lewis Research Center Group, Brook Park, Ohio 44142

An algebraic eddy-viscosity turbulence model based on the renormalization group formalism is presented with modifications to the baseline renormalization group model for wakes and separated flows. The renormalization group model is functionally the same as a mixing length model but requires neither length-based near- and far-wall damping terms nor empirical boundary-layer transition models. The damping characteristics of the renormalization group model and its behavior in laminar-to-turbulent transition regions are briefly studied using results from a two-dimensional channel flow calculation. The modified renormalization group model is used to compute the three-dimensional mean flow in a low-speed axial compressor rotor and is validated by direct comparison with the popular Baldwin-Lomax algebraic turbulence model. The computed results show good agreement with blade boundary layer and radial flow experimental data. The development of the tip leakage vortex is well predicted, and the computed wake decay also compares favorably with recent experimental data.

Nomenclature

B = channel width
c = chord
D = diameter
d = $2n/B$
f = friction factor, $8\tau_{wall}/\rho\bar{u}^2$
L_f = mixing length
L_f^i = integral scale
n = normal direction
P = turbulence production
R = radius ratio, r/r_{tip}
Re_m = Reynolds number, $\bar{u}B/\nu_0$
Re_t = Reynolds number, $u_{tip}D/\nu_0$
S = mean strain rate squared
s = distance from trailing edge
u = velocity
u^* = friction velocity, $\sqrt{\tau_{wall}/\rho}$
u^+ = u/u^*
$\bar{u}$ = average velocity, $\int u\,\delta n$
X = axial distance normalized by axial chord
y^+ = nu^*/ν_0
Z = surface arc length normalized by maximum length
δ = boundary-layer edge
ϵ = turbulence dissipation rate
κ = von Kármán constant
ν = renormalized or effective eddy viscosity
ν_0 = kinematic viscosity
ρ = density
τ = shear stress, $\nu S^{1/2}$
ϕ = flow coefficient, u_x/u_{tip}
ω = vorticity magnitude

Subscripts

r = radial
s = streamwise
t = transverse
tip = blade tip
x = axial

Presented as Paper 91-0172 at the AIAA 29th Aerospace Sciences Meeting, Reno, NV, Jan. 7-10, 1991; received Feb. 6, 1991; revision received Sept. 9, 1991; accepted for publication Sept. 14, 1991.

*Supervisor, Turbomachinery Analysis Section. Member AIAA.

Introduction

CLOSURE of the Reynolds averaged Navier-Stokes equations requires a model for the turbulence. For computational efficiency and code simplicity, many researchers use algebraic turbulence models; the most popular by far is that developed by Baldwin and Lomax.[1] In general, algebraic models are based on Prandtl's mixing length, which requires damping terms to mimic near-wall behavior and far-wall intermittency. In addition, mixing length models require highly empirical boundary-layer transition models. However, a formal analysis of turbulence can be applied that removes the reliance on empiricism found in most algebraic models for such phenomena as near-wall damping of turbulence, transition, and intermittency.

Such an analysis has been performed by Yakhot and Orszag.[2] Using the renormalization group (RNG) formalism, they were able to eliminate systematically the small scales of turbulence up to the resolvable scale and include the effects of the removed scales through an effective or renormalized viscosity. The RNG procedure begins by writing the full Navier-Stokes equation in Fourier space and decomposing the dependent variable into low and high wave number components rather than mean and fluctuating components, as is done in Reynolds averaging. By virtue of the correspondence principle (see Ref. 2), boundary conditions are removed from the analysis and small-scale stirring is used to recover a statistically equivalent system in the inertial range. Thus, the analysis is completely general. The stirring facilitates the renormalization procedure but does not produce large-scale nonlinearities upon averaging. The effect of large-scale structures can be introduced through a large eddy simulation or, as is the case here, by relating the smallest resolvable scale to a known flow parameter, such as the computed boundary-layer thickness. The unresolvable high wave number scales are eliminated through a complex mathematical process that assumes that the turbulence energy follows the $-5/3$ law in the inertial range and decays exponentially past some ultraviolet cutoff. The elimination of infinitesimally thin, high wave number bands is repeated over the renormalized spectrum, giving rise to recurrence relations that link the low Reynolds number regions of the turbulence with the high. Some constants appear in these relations but are determined analytically from assumptions about the shape of the energy spectrum. These constants are in good agreement with those determined experimentally but are not a function of problem dimensions or boundary conditions.

Recently, Martinelli and Yakhot[3] used an RNG-based algebraic eddy-viscosity model to compute the two-dimensional mean flow about an airfoil at angle of attack with very good results. Lund[4] used a similar model to study boundary-layer transition with very encouraging results. The purpose of this paper is to apply the RNG-based model in Ref. 3 to a complex three-dimensional flow and include modifications for wakes and separated flows. The viability of the RNG model as a useful engineering tool is assessed by calculating a low-speed compressor rotor flow, which is characterized by highly three-dimensional boundary layers, endwall vortices, and a tip leakage vortex. A direct comparison with experimental data and results using the Baldwin-Lomax model is made for validation purposes.

Renormalization Group Based Algebraic Model

In Ref. 2, the following relation for the renormalized viscosity is derived:

$$\nu = \nu_0\left[1 + H\left(\frac{a}{\nu_0^3}\epsilon\Lambda_f^{-4} - C_c\right)\right]^{1/3} \tag{1}$$

where $H(x)$ is the Heaviside function, which is zero for negative x and equal to x for all positive x. Λ_f is a suitably chosen infrared cutoff wave number in the spectrum of turbulence corresponding to the largest allowable scale in the inertial range. Assuming local equilibrium, ϵ is determined from Eq. (2a):

$$\epsilon = P = \nu S \tag{2a}$$

where

$$S = \left(\frac{\partial u_i}{\partial x_j} + \frac{\partial u_j}{\partial x_i} - \frac{2}{3}\delta_{ij}\frac{\partial u_k}{\partial x_k}\right)\frac{\partial u_i}{\partial x_j} \tag{2b}$$

The RNG model is now termed "energy based" through the use of Eq. (2a). This is an extremely attractive feature since mechanisms other than mean strain that generate turbulence can be included through simple modifications to Eq. (2a). As derived in Ref. 2 from the $-5/3$ power law for the turbulence energy spectrum, the coefficient a equals 0.1186 and C_c has the following form:

$$C_c = a/\gamma^4 \tag{3}$$

where γ corresponds to the wave number at the ultraviolet dissipation range cutoff in the spectrum of turbulence. This cutoff is near peak dissipation but within the inertial range and lies between $0.15 \le \gamma \le 0.2$, which gives a range of C_c roughly between 75 and 200. The choice of C_c is discussed later.

For large eddy simulations, the RNG model in Eq. (1) is used by relating the infrared cutoff wave number Λ_f to the integral length scale L_f^i by

$$L_f^i = \frac{2\pi}{\Lambda_f} \tag{4}$$

Then, the integral scale is set to the width of a suitably chosen Gaussian filter corresponding to the mesh size (see Ref. 2).

For the steady flow calculations performed here, L_f^i must be related to a mixing length L_f, which is done by ensuring that the high Reynolds number limit of Eq. (1) gives the familiar form of the Prandtl mixing length model, i.e.,

$$\nu = L_f^2 S^{1/2} \tag{5}$$

which neglects ν_0 because $\nu \gg \nu_0$ for high Re. Thus,

$$L_f = \frac{a^{1/4}}{2\pi}L_f^i \tag{6}$$

Therefore, in terms of a mixing length, Eq. (1) becomes

$$\nu = \nu_0\left[1 + H\left(\frac{\epsilon}{\nu_0^3}L_f^4 - C_c\right)\right]^{1/3} \tag{7}$$

For steady flow calculations, the effect of large-scale structures and boundary conditions are included by relating the mixing length to a parameter of the flow, such as the boundary-layer or displacement thickness. In this way, the RNG formalism, used primarily for large eddy simulations, is applicable to steady flows.

Solution Procedure

Since ϵ is a function of ν, we are left with a seemingly difficult solution of a cubic equation for the renormalized viscosity. However, the presence of the Heaviside function precludes imaginary roots. Thus, the roots can be determined using trigonometric relations, as in Ref. 5. With the Heaviside function in place, the locus of possible roots is displayed in Fig. 1. One can see that the cubic equation gives multiple allowable roots, i.e., real and greater than or equal to ν_0, in a small region bounded by $SL_f^4 = C_c\nu_0^2$ and $3\nu_0^2[(C_c - 1)/2]^{2/3}$. As a result, the choice of roots is unclear.

In Ref. 5, for simplicity, the maximum value of ν was chosen as the proper root. This choice yields a jump discontinuity in the distribution of ν from $\nu = \nu_0$ to $\nu = \nu_0[(C_c - 1)/2]^{1/3}$ when $SL_f^4 = 3\nu_0^2[(C_c - 1)/2]^{2/3}$. Lund[4] argues that, because such a jump is nonphysical, it is not representative of a laminar-to-turbulent transition process. To remove this discontinuity, Yakhot,[6] and then Lund,[4] recast the cubic into a quartic, which is solved using previous values of ν to determine which branch should be used. In addition, Lund[4] uses the undamped high Reynolds number limit of ν as an additional check. In Ref. 5, the jump discontinuity was considered a reasonable engineering approximation; however, the cubic

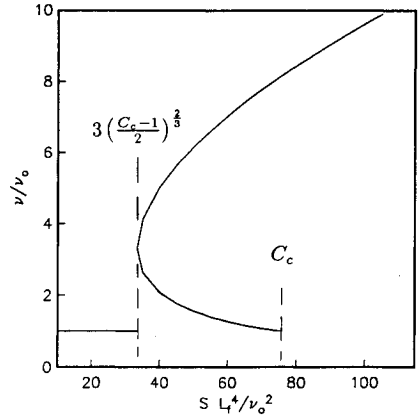

Fig. 1 Roots of the cubic for ν.

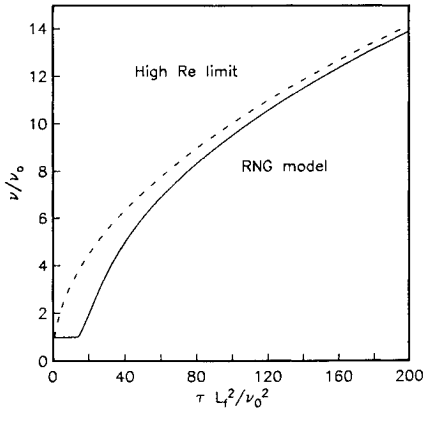

Fig. 2 Roots of the quartic for ν.

form of the equation could not be used for a certain transitional Reynolds number range for two-dimensional channel flow calculations. Therefore, following Yakhot[6] and Lund,[4] the cubic equation is cast as the following quartic:

$$\nu^4 - \nu\nu_0^3 - H(\tau^2 L_f^4 - \nu C_c \nu_0^3) = 0 \tag{8}$$

Equation (8) has two imaginary and two real roots, one negative and one positive. Only the latter is allowable since $\nu \geq \nu_0$. The most important feature of Eq. (8) is that it is single valued for all τL_f^2. The locus of allowable roots for Eq. (8) is displayed in Fig. 2 along with the high Reynolds number limit of $\nu = \tau^{1/2} L_f$. Clearly visible is the main attribute of the RNG-based algebraic model—its damping characteristics for small ν.

Equation (8) is now solved for ν using Newton's method with τ determined from previous values of ν. Convergence of four orders is usually achieved in two or three iterations. The renormalized viscosity is then included as an effective viscosity in a Navier-Stokes solver described in Ref. 7. The equations are cast in finite volume form and solved using a four-step Runge-Kutta time integration with a multigrid acceleration technique.

Attributes of the Renormalization Group Model

The most intriguing aspect of the RNG model is the capability of the Heaviside function and its argument to mimic a wide range of physical phenomena. If Eq. (8) is cast in inner variables (see Ref. 3), then the Heaviside function is zero for all $y^+ < (C_c^{1/4}/\kappa)$, which for $C_c = 200$ and $\kappa = 0.41$, gives $y^+ = 9.2$. This result lies within the transition region between the edge of the viscous sublayer and the beginning of the log law region. Furthermore, from Eq. (8), one can see that, as the edge of the shear layer is approached, τ tends to a small value so that $H(x)$ tends to zero in the outer layer. The Baldwin-Lomax model requires the addition of a Klebanoff intermittency factor to achieve the same damping along with a van Driest[8] damping term for proper near-wall behavior. Thus, the Baldwin-Lomax model is termed "length based."

The near-wall damping characteristics of the RNG model are illustrated with a simple two-dimensional channel flow calculation. Using Re_m of roughly 10^5, a simulation was run using both the RNG model and the simple Prandtl mixing length model, see Eq. (5). The length scale for both models is

$$L_f = 0.1435 - 0.082(1-d)^2 - 0.0615(1-d)^4 \tag{9}$$

which is based on Nikuradse's[9] result for smooth pipes at high Re.

In the limit of small d, Eq. (9) gives $L_f = 0.41d$. For the simple Prandtl mixing length model, proper near-wall behavior is achieved only by multiplying L_f by the van Driest damping term $(1 - e^{-y^+/26})$. The results of the calculations are plotted in inner variables in Fig. 3.

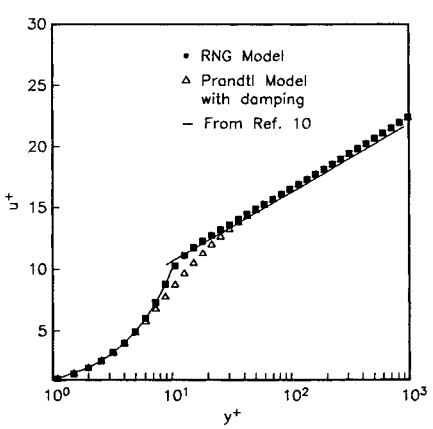

Fig. 3 Near-wall behavior of the RNG model.

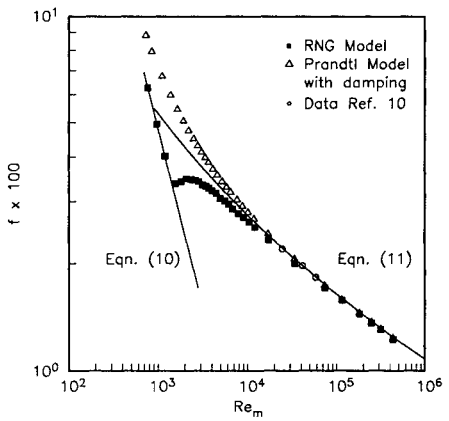

Fig. 4 Effect of Reynolds number on channel flow skin friction.

It is evident that both models properly predict the log law from the data of Hussain and Reynolds.[10] Without any length-based near-wall damping, the RNG model properly captures the viscous sublayer. Because of the character of the Heaviside function, a buffer region between the fully turbulent and the viscous-dominated regions is not recovered. However, this lack of a buffer is not a drawback and follows from the formally derived functional form of the RNG model. The value of y^+ where the Heaviside function becomes nonzero should then be close to the intersection of the $u^+ = y^+$ and log law curves. This intersection fixes C_c to a value near 200 for $\kappa = 0.41$. Clearly, the RNG model recovers the near-wall and log law behavior found experimentally.

An additional attribute of the RNG model is its ability to mimic the boundary-layer transition process. The Heaviside function suppresses deviations from laminar viscosity until the length scale and mean strain grow to values above the C_c cutoff. The same result occurs for turbulent-to-laminar transition, which is important in turbomachinery calculations because the pressure side of rotor blades is often transitional along the entire chord.

A simple study of the mimicry of boundary-layer transition can be made using the two-dimensional channel results by varying the Reynolds number. Assuming fully developed flow, the Reynolds number Re_m was varied from $\mathcal{O}(10^2)$ to $\mathcal{O}(10^6)$. In the laminar region, the friction factor f behaves as

$$f = 48/Re_m \tag{10}$$

In the turbulent region, integration of the log law with constants of integration set according to the experimental data of Ref. 10 gives

$$\frac{1}{\sqrt{f}} = 1.986 \log(Re_m \sqrt{f}) - 0.353 \tag{11}$$

These two curves are plotted along with the RNG and mixing length results in Fig. 4. The RNG model correctly mimics the transition from laminar to turbulent flow, whereas the mixing length model with van Driest damping cannot recover laminar flow except in the limit of very small Re_m. The Baldwin-Lomax model produces results identical to the mixing length results. The RNG model predicts transition at a Reynolds number based on the centerline velocity of 600. Two-dimensional linear stability analyses give a critical Reynolds number of roughly 5770 while early experimental data and a recent three-dimensional linear stability ananlsys yield a critical Reynolds number near 1000 (see Ref. 11). This early transition is due to the prescribed length scale, which is only a function of the channel width and not the flow. In Ref. 12, calculations of transitional flow by A. Yakhot using a length scale based on momentum and displacement thicknesses show the proper quantitative behavior. Other algebraic models use

empirical transition models, which can be awkward to use in multiple wall configurations.

A final attribute is that, due to the presence of ϵ in Eq. (7), nonequilibrium effects can be introduced through manipulation of Eq. (2a). The modification for separated flow made in the following section can be thought of as a nonequilibrium adjustment to ϵ. Additional modifications to Eq. (2a) can include the effects of buoyancy, streamline curvature, pressure gradient, and rotation, to name a few. Also, composite length scales can be used that are specifically tailored to the flowfield in question without regard to the character of the near- and far-wall damping since these effects are already built into the RNG model through the Heaviside function.

Determination of the Length Scale

In Ref. 3, the mixing length of turbulence L_f is set to the very familiar κn near solid boundaries, and $C_\mu\delta$ near δ. κ and C_μ can take on their established empirical values of 0.41 and 0.09, respectively, or their RNG-derived values of 0.372 and 0.0845, which is done here. Reference 3 uses the harmonic average of these inner and outer length scales in the following way:

$$L_f = \left(\frac{1}{\kappa n} + \frac{1}{C_\mu \delta}\right)^{-1} \tag{12}$$

A preferable length scale might be the following:

$$L_f = C_\mu \delta \tanh\left(\frac{\kappa n}{C_\mu \delta}\right) \tag{13}$$

which is used for all subsequent calculations. These length scales are compared in Fig. 5, where it is evident that Eq. (12) produces a length scale that is too small in the outer layer. The length scale and C_c are the only free parameters in the algebraic RNG model; the coefficients are determined analytically.

Determination of the Boundary-Layer Edge

One of the biggest problems in using an algebraic eddy-viscosity model is in determining the boundary-layer edge, which is required in Eq. (13). The method described by Baldwin and Lomax,[1] finding the peak of their function $F = n\omega$, is good for simple shear flows. However, complex shear layers are known to give several peaks in the distribution of F, as the examples in Ref. 1 attest. Finding the correct peak is not straightforward, at least in terms of coding. Often the second peak is arbitrarily chosen, but transients and three dimensionality can obscure the proper peak. Moreover, in many three-dimensional flows, streamwise vortical flows may lie just above or be embedded in the boundary layer, which further complicates the determination of the edge. The method chosen here is to use the point of maximum negative slope of F as the edge of the boundary layer. When applied to the examples in Ref. 1, the method yields the proper edge distance. In addition, the total vorticity in the determination of F is replaced with a vorticity magnitude without the streamwise component of vorticity. This method is very easy to code and has been found to work extremely well for a wide range of flows. In three dimensions, as with the Baldwin-Lomax model, the length scale is determined based on the value for the nearest wall.

Modification for Wakes

In the wake region of turbomachinery flow, the length scale L_f is determined from a correlation derived by Raj and Lakshminarayana.[13] The wake width from centerline to edge is first given by

$$b = \delta_0 + cC_d^{1/2}\, 1.35\left(\frac{s}{c} + 0.02\right)^{0.58} \tag{14}$$

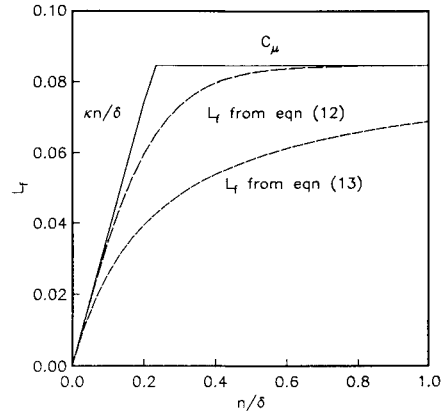

Fig. 5 Length scale for turbomachinery simulation.

Then,

$$L_f = \min(\kappa s, C_w b) \tag{15}$$

where δ_0 is the average of the pressure side and suction side boundary-layer thicknesses at the trailing edge, and C_d is the coefficient of drag, which can be computed based on the flow results. A design or best guess value is sufficient; and so C_d is usually set to 0.015 for compressors and 0.022 for turbines.

The first term in Eq. (15) is used to reduce the length scale very near the trailing edge. If the wake is assumed to be Gaussian, correlations for wakes behind circular cylinders yield a value of 0.169 for C_w. The advantage of using the correlation in Eq. (14) is that the wake centerline and wake width need not be found. Even if Eq. (15) is used in the Baldwin-Lomax model, the wake centerline needs to be found in order to evaluate the Klebanoff intermittency factor.

Enhancement for Separated Flows

Simpson et al.[14] indicate that the turbulence energy in the backflow region of a separated flow comes from diffusion and is not generated through the local mean strain, and so $P \neq \epsilon$. Therefore, the RNG model must be modified slightly to mimic the physics in this region properly. Note that even with all of the formalism in the RNG procedure, the degeneration to an algebraic form with all of the accompanying assumptions gives an equation that at times misrepresents the actual physical processes in special cases like separated flows. Following Simpson et al.,[14] the turbulence velocity scale in the backflow region is determined from the maximum shear stress in the outer flow. This velocity scale is included in Eq. (8) by replacing the local value of τ in the backflow region with $\tau_{\max}$ as determined in the outer flow.

Results and Discussion

To test the RNG-based turbulence model for complex three-dimensional shear layers, the flow in a low-speed axial flow compressor rotor at $Re_t = 3.4 \times 10^6$ is computed. The compressor rotor has 21 blades, operates at 1080 rpm, and has hub and shroud radii of 0.233 and 0.467 m, respectively, with a clearance gap of 2.0–2.5 mm. The computational mesh includes 88 cells in the axial direction and 44 in the radial and tangential directions. The mesh is concentrated near walls so that, on average, the first cell is at a y^+ of 5 on the blades and 20 on the endwalls. Only four cells are used in the tip clearance region. Tip clearance is modeled in a simplistic way by assuming the flow to be periodic in the gap region across single control volumes that span the blade thickness. The strength of the leakage jet and the vortex rollup are controlled by the Navier-Stokes equation and boundary conditions.

The flow is computed for a flow coefficient of $\phi = 0.50$ (peak pressure rise). Total CPU time required to reduce the residuals four orders of magnitude is roughly 12 h on the NAS Cray-YMP at NASA Ames Research Center.

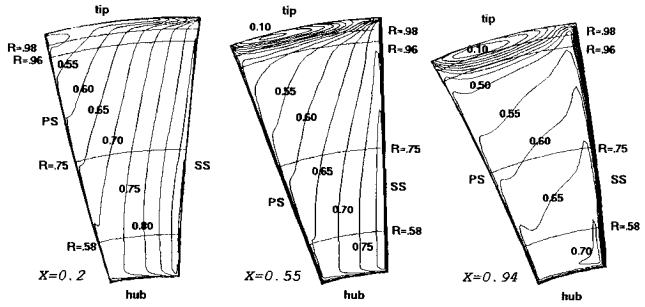

Fig. 6 Flow development in the rotor passage, contours of u_{total}/u_{tip}.

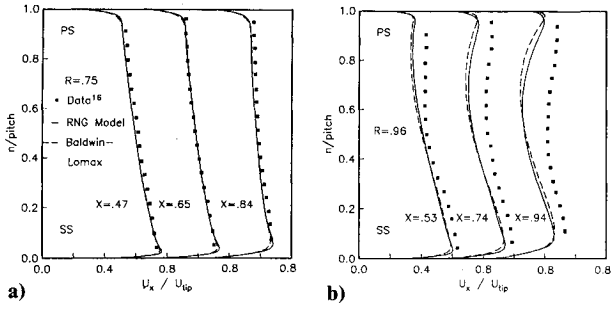

Fig. 7 Blade-to-blade axial velocity distribution.

The boundary-layer data were taken with a miniature hot-wire probe at several radii and axial stations by Lakshminarayana and Popovski.[15] It should be noted that near-wall data are very difficult to take and are subject to wall effects. Therefore, although corrected for these effects, the data very near the wall are subject to the largest error. In addition to the boundary-layer data, Popovski and Lakshminarayana[16] also measured blade-to-blade velocity profiles using laser anemometry.

Before proceeding with the direct comparison of computational results with the experimental data, it is instructive to examine the development of the flow in the blade passage. The reporting stations have been included with contours of total relative velocity at several axial locations in Fig. 6. The results in Fig. 6 are from calculations using the RNG turbulence model. At $X = 0.2$, the acceleration of flow along the suction side is evident, as is the strong leakage jet in the tip region. At $X = 0.55$, a leakage vortex begins to develop and influences the flow within 10% span from the tip. By the trailing edge, $X = 0.94$, the leakage vortex has fully developed and resides close to the shroud at roughly 60% pitch from the suction side and affects the flow almost 20% span from the tip. Notice that two reporting stations, $R = 0.96$ and 0.98, are deep in the very complicated leakage vortex region. In the hub region, a small passage vortex has developed but is confined close to the hub and not near the $R = 0.58$ reporting station.

The computed pitchwise distribution of axial velocity is compared to the experimental data at midspan and near the blade tip at $R = 0.75$ and 0.96, respectively. At $R = 0.75$, Fig. 7a, the results from the RNG model compare very well to results using the Baldwin-Lomax model and the experimental data at all axial locations. Near the blade tip at $R = 0.96$, Fig. 7b, the development of the leakage vortex is visible in both the data and the computational results by the velocity defect. The results using the Baldwin-Lomax model show the leakage vortex to be closer to the pressure side than the RNG results. It is clear from the data that, although the velocity defect is somewhat in error, the RNG results show the leakage vortex to be in the proper pitchwise location. It should be mentioned that, for simplicity, the length scale computed in the boundary layers is extended into the core region. Thus, this length scale may not be the proper scale for the leakage vortex, which is the reason for the slightly undermixed result.

The computed blade boundary-layer profiles are compared to the data and results using the Baldwin-Lomax model in Figs. 8–11 for various points along the blade surface. All velocities are normalized by the blade tip speed rather than by the edge velocities, which can hide inaccuracies. It is important to note that the results using the Baldwin-Lomax model were achieved by fixing the transition point at 10% c on the suction side and at the leading edge on the pressure side along the entire span. Using the transition criterion in Ref. 1 delayed transition too far downstream, giving poor agreement with the data. However, varying the transition location from 0 to 10% c did not significantly change the Baldwin-Lomax results. At midspan, the RNG model predicted a transition region near 12 and 17% c on the suction and pressure sides, respectively. Near the tip, the predicted transition points were near 6 and 25% c on the suction and pressure sides, respectively.

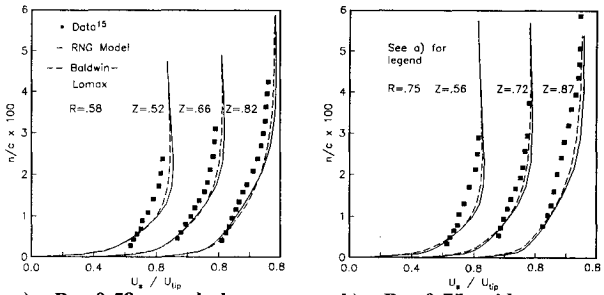

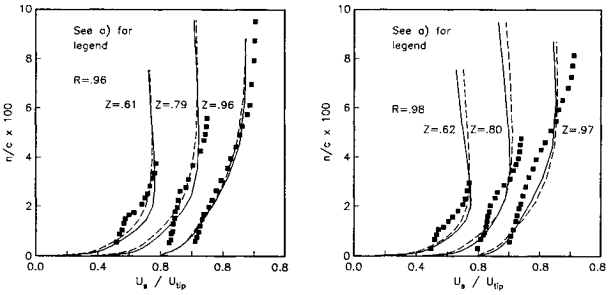

Fig. 8 Suction side streamwise velocity profiles.

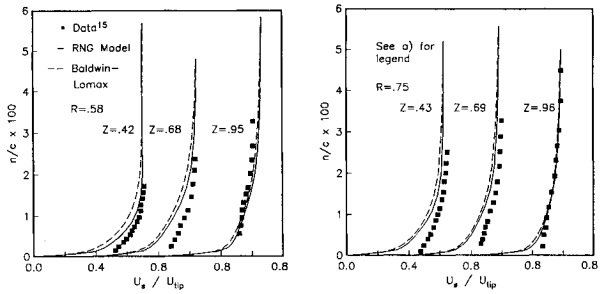

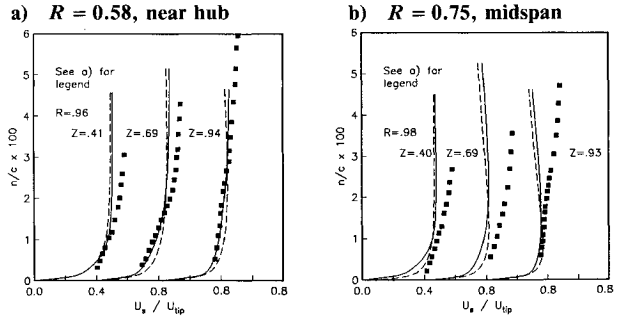

Fig. 9 Pressure side streamwise velocity profiles.

In all cases up to very near the blade tip, both algebraic models accurately compute the boundary-layer thickness and edge velocity. Streamwise velocity profiles on the suction side at various streamwise and radial locations are plotted in Fig. 8. At $R = 0.58$ near the hub, and $R = 0.75$ at midspan, the boundary-layer growth is accurately captured; however, the data indicate a more turbulent boundary layer than that computed by both models. The lack of agreement in the outer region is most likely due to the effect of rotation on the turbulence, which is not included in either model. This conclusion is based on results of a three-dimensional boundary-layer calculation performed by Zhang and Lakshminarayana.[17] Their results using isotropic eddy-viscosity models show almost identical results to those presented here; however, using an anisotropic algebraic Reynolds stress model (ARSM) that includes rotation terms, their results matched the experimental data.

Near the blade tip, the tip leakage flow influences the boundary-layer growth and shape. The different position of the leakage vortex from the Baldwin-Lomax and RNG models is the reason for the differences seen in Figs. 8c and 8d. The superiority of the RNG model over the Baldwin-Lomax model is subject to interpretation, and the reader is reminded that the comparison is made mostly for validation purposes. For both models, the overall error is still acceptable considering the coarseness of the mesh, for which roughly 14 cells define the boundary layer, and the assumptions of local equilibrium and isotropy.

The pressure side boundary layers are plotted at several radial and streamwise locations in Fig. 9. At $R = 0.58$ and 0.75, the RNG model performs slightly better than the Baldwin-Lomax model, especially near midchord. The trailing-edge velocity profiles from both models match the data very well. At $R = 0.96$, Fig. 9c, the RNG results compare more favorably with the data than the Baldwin-Lomax results, particularly at $Z = 0.69$ and 0.94. It is clear from the results near the tip that the leakage vortex computed from the Baldwin-Lomax model is too close to the pressure side and has thinned the pressure side boundary layer considerably. Finally, at $R = 0.98$, Fig. 9d, neither model performs very well, particularly in the outer flow region where the boundary-layer thickness is severely underpredicted.

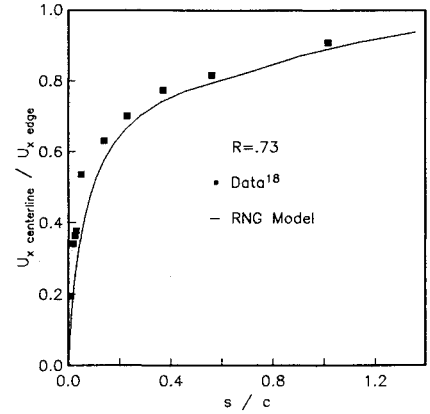

Fig. 12 Wake centerline axial velocity distribution.

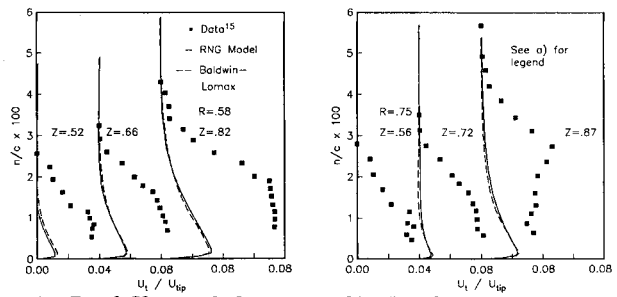

a) $R = 0.58$, near hub **b) $R = 0.75$, midspan**

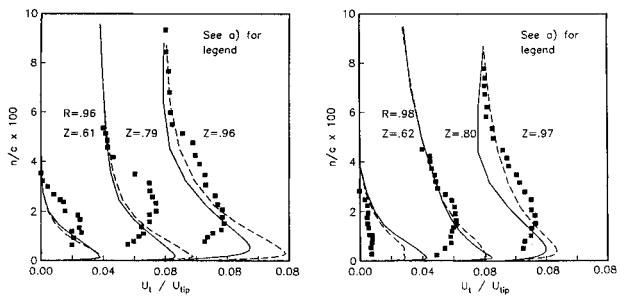

c) $R = 0.96$, near tip **d) $R = 0.98$, near tip**

Fig. 10 Suction side transverse velocity profiles.

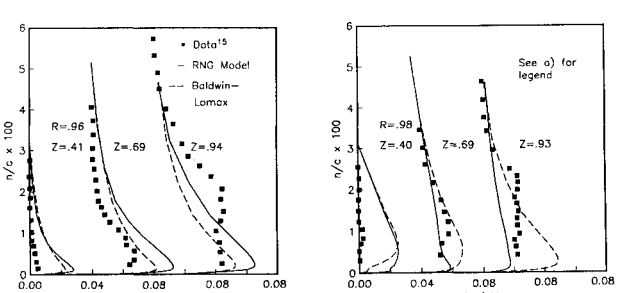

a) $R = 0.96$, near tip **b) $R = 0.98$, near tip**

Fig. 11 Pressure side transverse velocity profiles.

The transverse velocity profiles for the suction side are plotted in Fig. 10 at the same radial and streamwise locations as in Fig. 8. Both the RNG and Baldwin-Lomax models severely underpredict the magnitude of the radial flow at $R = 0.58$ and 0.75. The reason for such poor results is most likely grid resolution. The spanwise flow on compressor rotor blade surfaces is due to an imbalance between the radial pressure gradient and the centrifugal force from the whirl speed. This centrifugal force is directly related to the near-wall streamwise velocity gradient, which is underpredicted using both models, as seen in Fig. 8. Because three times the number of mesh points were used within the shear layer with commensurately better spanwise velocity profiles in Ref. 17, mesh resolution appears to be unsatisfactory for both models here. At $R = 0.96$, predictions improve in magnitude; however, neither model captures the character of the experimental transverse flow distribution close to the wall. Near the blade tip, $R = 0.98$, the transverse velocity profiles show similar disagreement very close to the wall. Still, both models perform similarly, which implies that disagreements with the experimental data are due to common assumptions that yield the algebraic form of the turbulence model. The simple tip clearance model used in the calculation also contributes to the error in the profiles very near the tip.

The transverse velocity profiles on the pressure side at $R = 0.96$ and 0.98 are plotted in Fig. 11. At $R = 0.96$, the results from both models are in qualitative agreement with the experimental data, although the near-wall values are too large due to the thickness of the computed pressure side boundary layer and resultant high shear stress, see Fig. 9. At $R = 0.98$, the two models give very different results; however, the RNG results are closer to the data near the wall. This good agreement with the data at $R = 0.98$ should be considered fortuitous due to the relatively poor agreement of the streamwise velocity profiles with the data on the pressure side near the tip.

Finally, the computed wake decay is compared to recent five-hole probe data taken by Prato[18] at $R = 0.73$ in Fig. 12. It is clear that the RNG model with the length scale correlation accurately captures the wake decay near midspan. Recall that the correlation is used only to determine the turbulence length scale and not the actual wake width. The decay rate is calculated very accurately and the magnitude of the wake defect is only 2% in error with the data. This result indicates that

higher order turbulence models may not be required to compute a rotor wake properly, provided a reasonable description of the turbulence length scale is included. Because the wake model described by Baldwin and Lomax[1] was not included in this calculation, no comparison with the RNG model is made.

Conclusions

The algebraic turbulence model based on the renormalization group formalism is a viable alternative to traditional algebraic models for complex three-dimensional flowfields. The results of a compressor rotor flow calculation show that, although the widely used Baldwin-Lomax algebraic turbulence model gives very good results, the RNG-based model using theoretically derived constants performs equally well without empirically derived length-based damping functions or transition models. In the blade tip region where the flow is highly three dimensional, the RNG model yields the proper location of the tip leakage vortex and gives commensurately better boundary-layer predictions than the Baldwin-Lomax model. An enhancement for separated flow was made to the model without destroying its functional character. In addition, a simple length scale correlation for cascade wakes was applied, which led to an accurate wake decay simulation. This result is very important to those studying unsteady rotor-stator wake interactions and other multistage effects. As indicated by previous work, the boundary-layer predictions using both turbulence models can be improved by using a finer mesh and a model for the anisotropy of the turbulence due to rotation.

As demonstrated in a two-dimensional channel flow calculation, the RNG model correctly mimics the boundary-layer transition process as well as the near-wall character of a fully turbulent boundary layer. Unfortunately, the ability of the RNG model to mimic transition in a complex turbomachinery flow was not adequately demonstrated in the compressor rotor computed here. A more difficult challenge is the prediction of transition on a turbine blade, which will be attempted in the future. With this validation, it seems that the RNG-based algebraic turbulence model properly represents the important physics of three-dimensional turbulent flows and has the potential to be a useful engineering tool that does not rely on experimental empiricism.

Acknowledgments

This work was supported by NASA Lewis Research Center under Contract NAS3-25266, with J. Adamczyk as monitor. Special thanks are given to M. Barton, V. Yakhot, R. Rubinstein, and P. Giel for valuable contributions. As always, K. Dugas is acknowledged for her skill in reviewing this manuscript.

References

[1]Baldwin, B. S., and Lomax, H., "Thin Layer Approximation and Algebraic Model for Separated Turbulent Flows," AIAA Paper 78-257, Jan. 1978.

[2]Yakhot, V., and Orszag, S. A., "Renormalization Group Analysis of Turbulence. I. Basic Theory," *Journal of Scientific Computing*, Vol. 1, No. 3, 1986, pp. 3–51.

[3]Martinelli, L., and Yakhot, V., "RNG-Based Turbulence Transport Approximations with Applications to Transonic Flows," AIAA Paper 89-1950, June 1989.

[4]Lund, T. S., "Application of the Algebraic RNG Model for Transition Simulation," *Instability and Transition*, edited by M. Y. Hussaini and R. G. Voigt, Vol. 2, Springer-Verlag, New York, 1990, pp. 463–479.

[5]Kirtley, K. R., "An Algebraic RNG-Based Turbulence Model for Three-Dimensional Turbomachinery Flows," AIAA Paper 91-0172, Jan. 1991.

[6]Yakhot, V., private communication, 1990.

[7]Kirtley, K. R., Beach, T. A., and Adamczyk, J. J., "Numerical Analysis of Secondary Flow in a Two-Stage Turbine," AIAA Paper 90-2356, July 1990.

[8]van Driest, E. R., "On Turbulent Flow near a Wall," *Journal of the Aeronautical Sciences*, Vol. 23, Nov. 1956, pp. 1007–1011.

[9]Nikuradse, J., "Gesetzmässigkeit der Turbulenten Strömung in glatten Rohren," VDI-Forschungsheft, No. 356, 1932.

[10]Hussain, A. K. M. F., and Reynolds, W. C., "Measurements in Fully Developed Turbulent Channel Flow," *Journal of Fluids Engineering*, Dec. 1975, pp. 568–580.

[11]Orszag, S. A., and Patera, A. T., "Subcritical Transition to Turbulence in Plane Channel Flows," *Physical Review Letters*, Vol. 45, No. 12, 1980, pp. 989–993.

[12]Yakhot, V., "Renormalization Group for Modelling of Turbulent Flows and Turbulent Combustion," AIAA Paper 91-0218, Jan. 1991.

[13]Raj, R., and Lakshminarayana, B., "Characteristics of the Wake Behind a Cascade of Airfoils," *Journal of Fluid Mechanics*, Vol. 61, Pt. 4, 1973, pp. 707–730.

[14]Simpson, R. L., Chew, Y. T., and Shivaprasad, B. G., "The Structure of a Separating Turbulent Boundary Layer. Part I. Mean Flow and Reynolds Stresses," *Journal of Fluid Mechanics*, Vol. 113, 1981, pp. 23–51.

[15]Lakshminarayana, B., and Popovski, P., "Three-Dimensional Boundary Layer on a Compresor Rotor Blade at Peak Pressure Rise Coefficient," *Journal of Turbomachinery*, Vol. 109, Jan. 1987, pp. 91–98.

[16]Popovski, P., and Lakshminarayana, B., "Laser Anemometer Measurements in a Compressor Rotor Flowfield at Off-Design Conditions," *AIAA Journal*, Vol. 24, No. 8, 1986, pp. 1337–1345.

[17]Zhang, J., and Lakshminarayana, B., "Computation and Turbulence Modeling for Three-Dimensional Boundary Layers Including Turbomachinery Rotors," *AIAA Journal*, Vol. 27, No. 11, 1990, pp. 1861–1869.

[18]Prato, J., "Effects of Blade Loading on the Wake Characteristics of a Compressor Rotor Blade," M.S. Thesis, Aerospace Dept., Pennsylvania State Univ., University Park, PA, Dec. 1990.